

Discovery Prospects of an Almost Fermiophobic W' in the Three-Site Higgsless Model at the LHC

Fabian Bach* and Thorsten Ohl†

*Institut für Theoretische Physik und Astrophysik,
Universität Würzburg, Hubland Nord, 97074 Würzburg, Germany*

(Dated: June 22, 2022)

Abstract

In extensions of the Standard Model with compactified extra dimensions, perturbative unitarity of the longitudinal gauge bosons is maintained through the contribution of heavy KK excitations of the gauge fields, without the necessity of introducing a Higgs field. The *Three-Site Higgsless Model* represents a minimal approach in this respect, containing just one extra set of heavy gauge bosons Z'/W'^{\pm} in the spectrum. While the Z' can have robust couplings to SM fermions and hence may be detected within the first $1\text{--}20\text{ fb}^{-1}$ of LHC data ($\sqrt{s} = 14\text{ TeV}$), the coupling of the W' to light fermions is suppressed and depends on the model parameters. Expanding on previous parton level studies, we determine discovery thresholds of the W' in s -channel Drell-Yan production at the LHC for masses $m_{W'} = 380, 500$ and 600 GeV , combining analyses of the semileptonic final states $\ell\ell jj$, $\ell\nu jj$ and the leptonic final state $\ell\nu\ell\ell$ ($\ell = e, \mu$) including fast detector simulation.

I. INTRODUCTION

The *Standard Model of Particle Physics* (SM) has been an extremely successful theory over the past decades, consistently explaining and predicting many different experimental results in high energy physics with unprecedented precision. While the experimental evidence for a breaking of the underlying local symmetry is unambiguous, the dynamics of this spontaneous breaking of the electroweak symmetry (EWSB) has not been accessible experimentally so far and remains an open question until now. Indeed, the *Large Hadron Collider* (LHC) at CERN has been designed to reach the electroweak breaking scale in hard parton scatterings and illuminate this yet unresolved question experimentally.

On the theoretical side, numerous approaches exist in the literature to implement a dynamical mechanism of symmetry breaking in the SM which also keeps the scattering of longitudinal gauge bosons unitary at high energies above 1 TeV [1–6], among which the introduction of a fundamental scalar Higgs field [4, 5, 7, 8] is only the most simple and straightforward one, albeit with some much-discussed theoretical drawbacks such as the quadratic dependence on the ultraviolet completion known as the *hierarchy problem*. Other approaches are, for example, technicolor models with an additional strongly interacting sector [9, 10], whose meson-like bound states play the role of the symmetry-breaking scalars, or models with one or more additional space-time dimensions compactified on the electroweak length scale [11–13], where symmetry breaking can be accounted for by non-trivial ground state configurations of the additional gauge field components.

Indeed, in the case of five dimensions with the geometry of a 5D Anti-de Sitter space, these different types of models turn out to be related to each other by a duality commonly addressed as AdS/CFT correspondence [12, 13]. The Three-Site Higgsless Model (3SHLM) [14] can be counted among this class of theories as a maximally deconstructed [15, 16] limit, thus representing an effective low energy theory parametrizing only the leading contributions of a more general higgsless 5D theory as a UV completion [17–20]. More explicitly, maximal deconstruction means that the extra dimension is discretized on just three sites, giving rise to the inclusion of only the first Kaluza-Klein (KK) excitations of the SM fields along the new dimension into the particle spectrum. While electroweak precision tests (EWPT) severely constrain the mass scale of the heavy fermions to $\gtrsim 2$ TeV, the masses of the heavy gauge bosons Z'/W'^{\pm} can be consistently chosen as low as 380 GeV [14, 21, 22], whereas an upper

limit around 600 GeV is dictated by the necessity to unitarize the scattering amplitudes among longitudinal gauge bosons. Although ideal delocalization allows to implement an exact vanishing of the W' coupling to SM fermions $g_{W'ff}$ at the tree level [14], the results of a one-loop analysis [21] actually favour small but finite couplings.

In view of the major LHC experiments currently gaining precision and improving bounds on new physics signatures literally every month, there is an ongoing interest in higgsless models predicting new gauge bosons with strongly suppressed couplings to SM fermions, making them hard to access experimentally. Even though there already exist quite a few studies dealing with the discovery prospects of such heavy gauge bosons [23–31] (the most recent one [31] discussing the LHC discovery reach of heavy charged gauge bosons $W_{1,2}^\pm$ in the Four-Site Higgsless Model, whose couplings are less constrained than in the 3SHLM), most of them are restricted to the parton level, which does not account for—possibly large—effects due to the detector response. Discovery limits for the Z' including detector effects have recently been reported elsewhere [32], but the discovery of the W' is crucial to distinguish the 3SHLM in the one-loop scenario from a generic Z' with suppressed couplings. This paper is focussing on the sensitivity to the W' in s -channel production. We compare the most promising final states $\ell\ell jj$, $\ell\nu jj$ and $\ell\nu\ell\ell$ ($\ell = e, \mu$) of a W' decaying predominantly into intermediate pairs of SM gauge bosons WZ in order to extract the most sensitive one at the detector level, also including an assessment of the method studied in [23] at parton level to distinguish the nearly degenerate W' and Z' resonances in the $\ell\nu jj$ channel. Note that, apart from the specific case discussed here, this method is in principle applicable to a more general class of signal patterns where resonances lie close together, especially when data analysis is further complicated, e. g. by information loss due to invisible particles in the final state.

This article is organized as follows: Section II is devoted to a brief review of the construction principles and parameter space of the 3SHLM, while in section III we point out the generation and detector simulation of the analyzed samples and present sensitivities and discovery prospects in the different channels mentioned. Finally, a summary and detailed discussion of the results can be found in section IV.

II. THE THREE-SITE HIGGSLESS MODEL

The 3SHLM [14] can be understood as an effective low-energy approximation of a 5D theory with one extra space dimension y of the size of the EWSB scale and a gauged 5D $\mathbf{SU}(2)$ bulk symmetry broken to a $\mathbf{U}(1)$ on one of the branes. In addition, y is maximally deconstructed, i.e. discretized to three sites only, so that only the ground states and the first KK excitations of the matter and gauge fields along y remain in the spectrum. In the effective 4D theory, this deconstruction corresponds to an extended electroweak gauge group

$$\mathbf{SU}(2)_0 \times \mathbf{SU}(2)_1 \times \mathbf{U}(1)_2, \quad (1)$$

where the chiral $\mathbf{SU}(2)_L \times \mathbf{U}(1)_Y$ symmetry of the SM is realized via boundary conditions breaking the full symmetry on the brane sites 0 and 2. In the limit $g_{0/2} \ll g_1$, the gauge couplings can be approximately identified as the electroweak SM couplings $g_0 \sim g$ resp. $g_2 \sim g'$, and any new physics contribution from site 1 will be suppressed as $g_{0/2}/g_1$.

In this setup, EWSB can be implemented by a non-trivial vacuum configuration of the y -component of the 5D gauge field $A_M(x)$ with $M = 0, 1, 2, 3, y$. In the deconstructed 4D picture, the component $A_y(x)$, i.e. the gauge connection between the sites, is mediated by two independent $\mathbf{SU}(2)$ -valued Wilson line fields $\Sigma_{0/1}(x)$ which transform bi-unitarily under gauge transformations as

$$\Sigma_0 \rightarrow U_0 \Sigma_0 U_1^\dagger, \quad \Sigma_1 \rightarrow U_1 \Sigma_1 e^{-i\theta\sigma_3/2} \quad (2)$$

with gauge group elements $U_i \in \mathbf{SU}(2)_i$ and $e^{-i\theta\sigma_3/2} \in \mathbf{U}(1)_2$. Choosing the minimal nonlinear sigma representation for the Wilson lines, the $\Sigma_i(x)$ become unitary and EWSB is realized by the vacuum expectation values

$$\langle \Sigma_{0/1} \rangle = \sqrt{2}v \quad (3)$$

(this symmetry breaking pattern is very similar to the BESS model [33]).

Together with eqn. (3), the kinetic terms of the $\Sigma_i(x)$ generate mass terms for the gauge fields, which upon diagonalization, and in the limit $g_{0,2} \ll g_1$ mentioned above, lead to a massless photon A and a light set of mass eigenstates W^\pm/Z mostly localized on the boundary branes (to be identified with the SM gauge bosons) as well as a heavy, almost degenerate set W'^\pm/Z' of mass $m' \sim g_1 v$ localized on the bulk site 1. The allowed range of

m' is

$$380 \text{ GeV} \lesssim m' \lesssim 600 \text{ GeV} , \quad (4)$$

where the lower bound comes from the LEP2 measurement of the triple gauge boson coupling g_{ZWW} [34, 35] and the upper bound is due to the requirement that the heavy gauge bosons be light enough to delay the violation of unitarity in longitudinal gauge boson scattering.

5D bulk fermion fields are broken up by deconstruction into independent fermion fields Ψ_i at each site i , whereas the chirality of the SM is enforced by boundary conditions, i. e. by requiring Ψ_0 to be a left-handed doublet under $\mathbf{SU}(2)_0$ and the $\Psi_2^{u/d}$ to be right-handed and singlets under all the $\mathbf{SU}(2)_i$, while the bulk fermions Ψ_1 remain fully left-right symmetric doublet representations of the $\mathbf{SU}(2)_1$. In addition, the $\Psi_{0/1}$ carry $\mathbf{U}(1)_2$ charges equal to the hypercharges of left-handed SM fermions, whereas the $\mathbf{U}(1)_2$ charges of the $\Psi_2^{u/d}$ are equal to the right-handed SM hypercharges. Mass terms are then generated by a combination of Yukawa couplings to the Σ fields and a gauge invariant Dirac mass term $M\bar{\Psi}_{1L}\Psi_{1R}$ which normalizes the overall mass scale:

$$\mathcal{L}_{\text{mass}} = M \left[\epsilon_L \bar{\Psi}_{0L} \Psi_{1R} + \bar{\Psi}_{1L} \Psi_{1R} + \bar{\Psi}_{1L} \begin{pmatrix} \epsilon_R^u \\ \epsilon_R^d \end{pmatrix} \begin{pmatrix} \Psi_{2R}^u \\ \Psi_{2R}^d \end{pmatrix} \right] + \text{h.c.} , \quad (5)$$

where the vev's of the Σ_i , eqn. (3), have been inserted and a sum over the three flavor generations is implied. In this parametrization, $M \gtrsim 2 \text{ TeV}$ is a universal heavy fermion mass scale, with the lower bound coming from heavy fermion loops contributing to the W propagator and hence affecting EWPT [14], and the $\epsilon_i \sim v/M$ are dimensionless delocalization parameters mixing fermions from adjacent sites.

Again, after diagonalization one finds a heavy set of fermions mostly living on the bulk site and a light set localized on the boundaries which is identified with the SM fermions. The SM flavor structure is incorporated in a minimal way, i. e. by fixing the matrices $\epsilon_R^{u/d}$ according to flavor phenomenology while keeping M and ϵ_L as universal, free parameters of the model (together with m'). However, ϵ_L is strongly correlated with m' in order to keep the model consistent with EWPT. More explicitly, the coupling $g_{W'ff}$ of the W' to SM fermions is straightforwardly given by the gauge couplings times the overlap of the wave functions of mass states on the respective sites

$$g_{W'ff} = g_0 (f_L^0)^2 v_{W'}^0 + g_1 (f_L^1)^2 v_{W'}^1 , \quad (6)$$

where the f_L^i and $v_{W'}^i$ are found in the diagonalization of the mass matrices and relate the mass states of the light left-handed fermions and the W' , respectively, to the corresponding interaction eigenstates on site i , with $f_L^0/f_L^1 \sim \epsilon_L$ and $v_{W'}^0/v_{W'}^1 \sim m_W/m'$ to leading order. At tree level, eqn. (6) is required to give exactly zero in order to protect the electroweak precision parameters from W' contributions, thus imposing a strict relation between ϵ_L and m' —a setup referred to as *ideal delocalization* [36] in [14]. However, as pointed out in [21], at one-loop level ideal delocalization turns out to be ruled out at 95 % c.l. in favor of a small but non-vanishing coupling $g_{W'ff}$ of the W' to the SM fermions, so that the search for a W' resonance in the s channel at the LHC will be sensitive not only to m' but also to ϵ_L and to M . In the present study, we will essentially rely on the 95 % c.l. allowed regions in the M - ϵ_L parameter plane given in [21] for fixed heavy gauge boson masses $m' = 380, 500$ and 600 GeV.

III. DISCOVERY POTENTIAL OF THE W' AT THE LHC

In this section, we present our results of a Monte Carlo-based feasibility study of the search for the resonance of a 3SHLM-like W' boson which is produced in the non-ideal delocalization setup via s channel quark annihilation. It predominantly decays into a pair of SM gauge bosons $W' \rightarrow WZ$, subsequently decaying into four-fermion final states, of which $\ell\ell jj$, $\ell\nu jj$ and $\ell\nu\ell\ell$ ($\ell = e, \mu$) are most promising due to moderate ($\ell\ell jj$, $\ell\nu jj$) or absent ($\ell\nu\ell\ell$) QCD backgrounds, whereas the purely hadronic final state $jjjj$ was not considered here due to the huge QCD background. The data generation and simulation setup of the study is designed to reproduce LHC-like proton–proton collisions at $\sqrt{s} = 14$ TeV and to approximately imitate the ATLAS [37] detector response via a fast detector simulation with smearing effects.

A. Data Generation and Detector Simulation

All signal and background samples have been produced with version 2 of the parton-level Monte Carlo event generator WHIZARD [38]. All final states containing up to four particles were generated using full tree level matrix elements including all off-resonant diagrams and irreducible backgrounds. This already covers most of the dominant QCD backgrounds

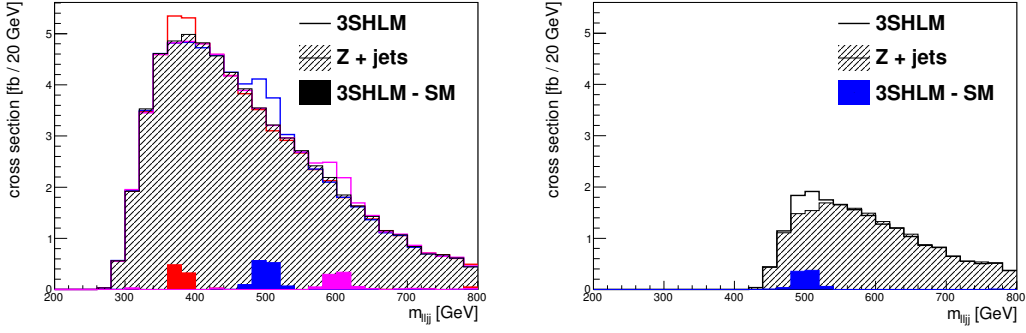


FIG. 1: Total invariant mass distribution of the final state $\ell\ell jj$ after all cuts without (l.h.s) and including (r.h.s.) the p_T cut on the SM gauge boson momenta, with maximal $g_{W'ff}$ allowed in the one-loop scenario and $m' = 380$ (red), 500 (blue) and 600 GeV (pink).

coming from W/Z plus one or two colored partons in the semileptonic channels. For the additional $t\bar{t}$ background in the $\ell\nu jj$ channel, the computational complexity has been reduced by selecting only those diagrams which contain two b quarks and two W boson propagators decaying semileptonically.

All WHIZARD output was then processed with PYTHIA [39] for showering and hadronization. Finally, detector effects have been accounted for using the fast detector simulation DELPHES [40] with the default ATLAS card shipped with the package. Calorimeter jets have been reconstructed with the anti- k_T algorithm [41] and cone size $R = 0.4$. Also b -tagging has been applied with an assumed efficiency of 0.6 [37] in order to suppress the $t\bar{t}$ background in the $\ell\nu jj$ channel.

B. The $\ell\ell jj$ Channel

The $\ell\ell jj$ channel is the most straightforward one, because all final state objects are visible in the detector, so that their momenta can in principle be uniquely determined from detector data. Moreover, this channel contains no Z' signal, thus conveying a clean signature to discriminate the one-loop scenario [21] from the ideal delocalization scenario [14], where the W' resonance should vanish completely.

For event selection, we require exactly two isolated, oppositely charged leptons as well as at least two hadronic jets all passing the kinematic cuts

$$p_T > 50 \text{ GeV} \quad \text{and} \quad |\eta| < 2.5 \quad (7)$$

together with a cut on the invariant di-lepton mass within ~ 2 FWHM around the Z mass:

$$|m_{ee} - m_Z| < 5 \text{ GeV} \quad \text{resp.} \quad |m_{\mu\mu} - m_Z| < 10 \text{ GeV} . \quad (8)$$

In order to further reduce QCD background, additional kinematic cuts are applied to the hadron jets, which restrict the allowed phase space to the topology associated with the decay of two strongly boosted SM gauge bosons. The corresponding requirements are to find a jet pair with an invariant mass within a cut window around the W mass and a relatively small enclosed angle,

$$|m_{jj} - m_W| < 10 \text{ GeV} \quad \text{and} \quad \Delta R(j, j) < 1.3 . \quad (9)$$

Finally, with the two lepton momenta and the momenta of the di-jet resonance, a p_T cut [32] as well as a back-to-back cut is applied on the reconstructed gauge boson momenta associated with the lepton pair and the jet pair:

$$p_T^{W/Z} > \begin{cases} 150 \text{ GeV}, & m' = 380 \text{ GeV} \\ 200 \text{ GeV}, & m' = 500 \text{ GeV} \\ 250 \text{ GeV}, & m' = 600 \text{ GeV} \end{cases} ,$$

$$\Delta R(W, Z) > 2.0 . \quad (10)$$

The signal observable is then given by the total invariant mass $m_{\ell\ell jj}$ of all four 4-momenta in the final state, where a veto is imposed on b-tagged jets passing $p_T > 25 \text{ GeV}$ and $|\eta| < 2.5$ cuts in order to further reduce background. (Particularly, $t\bar{t}$ background can be neglected when requiring two hard leptons reconstructing a Z in combination with a veto on b jets and missing transverse momentum.)

Significances are obtained by adding the reducible background samples to the signal as well as the SM contrast sample and evaluating the excess events in the resonance region normalized by the background fluctuation,

$$s = \frac{N_{\text{3SHLM}} - N_{\text{SM}}}{\sqrt{N_{\text{SM}}}} , \quad (11)$$

where the resonance region is chosen symmetrically around m' . Note that m' is assumed to be known within the 3SHLM from a discovery of the practically degenerate Z' , which must necessarily have taken place before any sensitivity to the W' in the s channel can be expected due to the much larger coupling. The width of the resonance window is adjusted

such that the value for the significance minus its statistical uncertainty is optimized. As illustrated in fig. 1, however, the $\ell\ell jj$ channel suffers greatly from the tiny signal together with large QCD backgrounds, giving e.g. a 5σ discovery threshold of $\int L \approx 150 \text{ fb}^{-1}$ at the most optimistic point of the parameter space ($m' = 500 \text{ GeV}$, max. $g_{W'ff}$ allowed), so that the possibility of a discovery in this channel remains questionable on the basis of this study, at least with more or less realistic assumptions on the total integrated luminosity to be delivered by the LHC.

C. The $\ell\nu jj$ Channel

This channel is somewhat more involved for a W' search than the previous one due to the missing kinematic information of the neutrino which escapes detection. Furthermore, the W' signal is superimposed with a large degenerate Z' resonance (cf. [32]), so that the possibility to extract the W' is closely linked to the ability to distinguish the heavy SM gauge boson resonances in the di-jet system [23]. These issues are addressed below in due order.

The selection criteria for this channel are very similar to those described in sec. III B for the $\ell\ell jj$ channel: we basically require at least two hard jets passing the kinematic cuts (7) together with an invariant mass cut

$$m_W - 20 \text{ GeV} < m_{jj} < m_Z + 20 \text{ GeV} , \quad (12)$$

which accounts for the fact that in the di-jet mass a small Z resonance coming from the W' is added to a large W resonance coming from a Z' . (The cut window is increased compared to (9) because of the discrimination procedure described below.) In addition, we require exactly one hard lepton passing the kinematic cuts (7) as well as missing transverse energy \cancel{E}_T larger than the p_T cut in (7), together with a b -jet veto as described in section III B in order to suppress the large $t\bar{t}$ background in this channel.

Reconstruction of the Neutrino Momentum

The momentum of the neutrino $p_\nu = p$ is reconstructed from the charged lepton 4-momentum $p_\ell = q$ in the usual way by identifying \cancel{E}_T with the neutrino p_T and using the

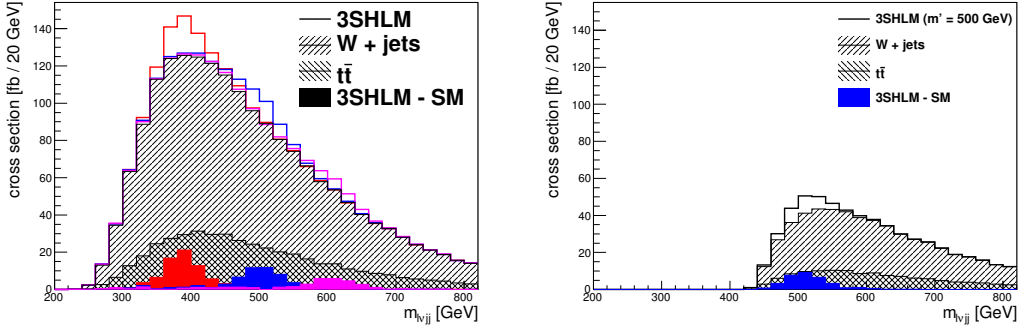


FIG. 2: Total invariant mass distribution of the final state $\ell\nu jj$ after all cuts without (l.h.s) and including (r.h.s.) the p_T cut on the SM gauge boson momenta, with maximal $g_{W'ff}$ allowed in the one-loop scenario and $m' = 380$ (red), 500 (blue) and 600 GeV (pink).

on-shell condition for the the intermediate W boson

$$(p + q)^2 = m_W^2 \quad (13)$$

with massless leptons to account for the missing information. In general, this quadratic equation has two solutions,

$$p_z = \frac{q_z (m_W^2 + 2\vec{p}_T \cdot \vec{q}_T) \pm q_0 \sqrt{D}}{2q_T^2} \quad (14)$$

with the determinant

$$D = (m_W^2 + 2\vec{p}_T \cdot \vec{q}_T)^2 - 4p_T^2 q_T^2,$$

so that we pick the solution with a lower $|p_z|$, following the argument in [32]. However, due to off-shell effects of the intermediate W and detector smearing, a reasonable amount of events (roughly 10 % at parton level and 25 % at detector level) fails to give a real solution altogether, namely when D becomes negative. In this case, in order minimize the loss of statistics, we use $D = 0$ as another condition and additionally solve for the invariant mass $m_{\ell\nu}$ of the leptonic W in the resulting equations, finally cutting on $m_{\ell\nu}$ corresponding to the mass cut in eqn. (9) to sort out unphysical results (cf. [42] for a more detailed discussion of the method). Numerically it turns out that roughly 10 % of the original number of events can be reconstructed this way with a competitive signal-to-background ratio in the resonance region, so that they are included in the analysis. Ultimately, having obtained a neutrino momentum and a corresponding W boson momentum, we also apply the p_T and

back-to-back cuts (10) on the leptonic and the hadronic resonances before computing the total invariant mass $m_{\ell\nu jj}$ of the final state (cf. fig. 2).

Disentangling the Jet Resonances

As mentioned above, an important feature of the $\ell\nu jj$ final state is that it encompasses the decay of both heavy gauge bosons with the same signature, so that the only means of signal discrimination is to disentangle the two SM gauge bosons in the di-jet resonance. At detector level, these resonances have widths of the order of the mass splitting itself, which makes it almost impossible to separate them merely by invariant mass cuts. This problem was addressed at parton level in [23], proposing a statistical method to numerically separate the two SM resonances and hence the two heavy resonances: The true gauge boson counts N_W and N_Z within a given sample are assumed to be smeared over a certain invariant mass range according to underlying probability density functions $p_i(m)$, which can be approximated by a convolution of the intrinsic Lorentz distribution with an experimental detector response function described by a Gaussian distribution. If the $p_i(m)$ are known at detector level, the signal mixture

$$\tilde{N}_i = \sum_j T_{ij} N_j, \quad i, j = W, Z \quad (15)$$

with

$$T_{ij} = \int_{L_i}^{U_i} dm p_j(m) \quad (16)$$

can be inverted numerically to infer the true numbers N_W and N_Z from the smeared numbers \tilde{N}_W and \tilde{N}_Z counted inside the mass windows

$$\begin{aligned} L_W &= 60 \text{ GeV} , \\ U_W &= L_Z = \frac{m_W + m_Z}{2} , \\ U_Z &= 111 \text{ GeV} . \end{aligned} \quad (17)$$

Whereas the authors of [23] assume an experimental Gaussian smearing of 10 GeV as an input in their parton level study, a different approach is chosen here: MC samples are produced at parton level which contain strongly boosted back-to-back W and Z bosons decaying hadronically, thus mimicking the final state topology of the signal. Then the clean

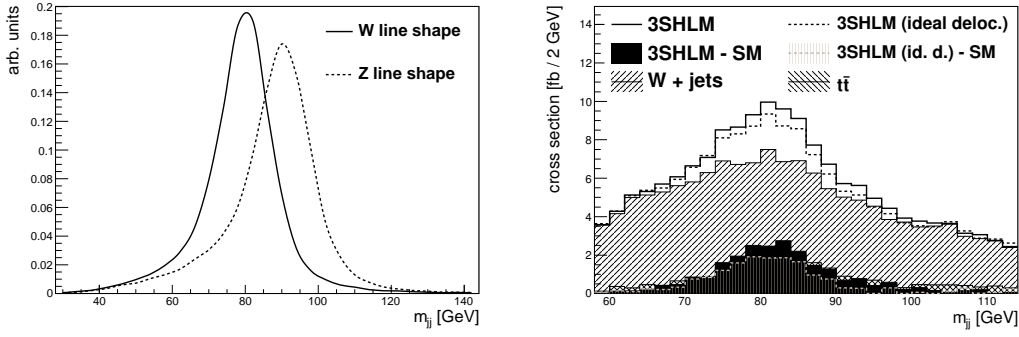


FIG. 3: Normalized line shapes of the di-jet resonances of boosted W and Z bosons at detector level (l.h.s). The r.h.s. shows the invariant di-jet mass distribution within the range of the SM bosons in the physical samples, after cutting on the resonant region around m' in $m_{\ell\nu jj}$.

W resp. Z resonance line shapes in the invariant di-jet mass obtained from these samples at detector level (cf. fig. 3) are used as an approximation for the unknown $p_i(m)$, from which the mixing matrix T and its inversion are then computed numerically using eqn. (16), giving

$$T^{-1} \approx \begin{pmatrix} 1.68 & -0.82 \\ -0.60 & 1.89 \end{pmatrix}. \quad (18)$$

Having determined the T_{ij}^{-1} , the relevant signal events are isolated by cutting on the total invariant mass $m_{\ell\nu jj}$ within a region of ± 30 GeV around the heavy resonance (cf. fig. 2), where $m' = 500$ GeV was chosen here for a feasibility test of the method, because a medium value of m' allows for the largest absolute values of $g_{W'ff}$ (cf. [21]) and hence possesses the highest discovery potential. After this cut, the SM gauge boson resonances are examined in the invariant mass distributions m_{jj} of the corresponding jet pairs (cf. fig. 3) in order to obtain the mixed numbers \tilde{N}_i inside the cut windows $\{L_i, U_i\}$ specified in eqn. (17), and finally apply T^{-1} . The whole procedure is carried out both with maximal $g_{W'ff}$ as well as in ideal delocalization for a cross check.

As detailed in table I, the Z significance, implying the decay of a W' , does indeed drop to nearly zero in ideal delocalization as expected, while a finite significance $s = 1.5$ remains with maximal $g_{W'ff}$. In the parton level analysis of [23] a significance $s \sim 2$ was found for the disentangled Z signal, whereas the basic differences between their analysis and this one are that the detector width of SM bosons in jet pairs was somewhat overestimated with 10 GeV, while, on the other hand, the considerably large background contributions of inclusive

| ideal delocalization | | | | | maximal $g_{W'ff}$ | | | | |
|----------------------|---------------|---------------|-------|-------|--------------------|---------------|---------------|-------|-------|
| i | \tilde{N}_i | \tilde{s}_i | N_i | s_i | i | \tilde{N}_i | \tilde{s}_i | N_i | s_i |
| W | 1203 | 6.8 | 1713 | 5.3 | W | 1533 | 8.6 | 1972 | 6.1 |
| Z | 373 | 2.5 | -21 | -0.07 | Z | 734 | 4.9 | 462 | 1.5 |

TABLE I: Signal events and significances as computed from eqn. (11) for $\int L = 100 \text{ fb}^{-1}$ before and after disentangling the signal as described in the text, in ideal delocalization (left) and with maximal W' coupling to SM fermions (right). The significance also drops for the W signals because the uncertainty generally becomes larger in the disentangling procedure.

jet production at the detector were underestimated at parton level. In any case, this result is still far away from a liable discovery threshold for an integrated luminosity of 100 fb^{-1} considered here, so that the discovery prospects for the W' remain very poor also in the $\ell\nu jj$ channel.

D. The $\ell\nu\ell\ell$ Channel

Another venue for a discriminative search for the heavy W' is the purely leptonic final state $\ell\nu\ell\ell$, which possesses by far the smallest cross section but at the same time a very clean detector signature compared to the semileptonic channels considered above. The event selection requirements are in this case exactly three isolated charged leptons passing the kinematic cuts in eqn. (7) as well as missing transverse momentum passing the p_T cut. The further procedure simply is to combine the treatments of one or two charged leptons discussed in the previous sections: With mixed flavors, the lepton pair of equal flavor is required to have opposite charges and the kinematic topology corresponding to the decay of a boosted Z boson, i. e. pass the invariant mass cut pointed out in eqn. (8), while the third lepton of different flavor is required to reconstruct at least one neutrino momentum together with an \cancel{E}_T (cf. the discussion in section III C) that also passes the kinematic cuts. With three leptons of equal flavor, the procedure is to demand mixed charges and pick from the two possible pairs of oppositely charged leptons the one whose invariant mass is closer to the Z mass, whereas the remaining lepton is then required to produce at least one reasonable neutrino momentum together with \cancel{E}_T . Finally, the reconstructed SM gauge boson momenta

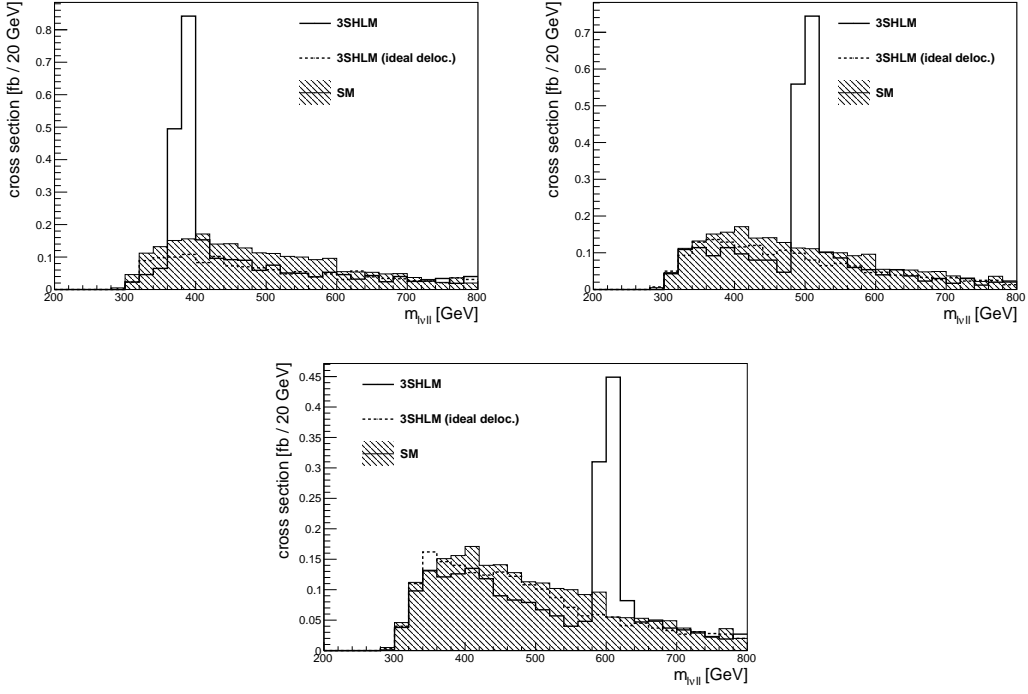


FIG. 4: Total invariant mass of the final state $l\nu ll$ in the SM as well as in the 3SHLM (ideal and non-ideal delocalization with max. $g_{W'ff}$ allowed) for $m' = 380, 500$ and 600 GeV (parton level).

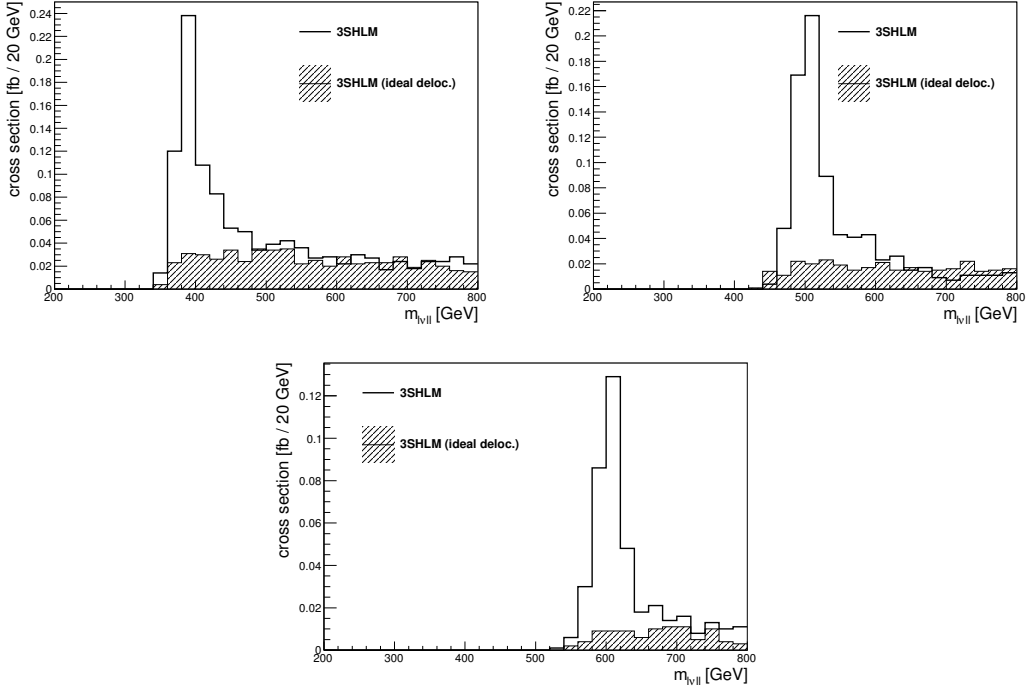


FIG. 5: Total invariant mass of the final state $l\nu ll$ in the 3SHLM (ideal vs. non-ideal delocalization with max. $g_{W'ff}$ allowed) for $m' = 380, 500$ and 600 GeV, including the p_T and back-to-back cuts on SM gauge bosons (10) (detector level).

should in any case also pass the p_T and back-to-back cuts given in eqn. (10).

In contrast to the other channels, in this case not only the signal but also the whole background is purely electroweak, so that sizeable interference terms with diagrams containing heavy bosons or fermions can be expected and are indeed present, qualitatively affecting the sideband shape around the resonance compared to the SM sample. Moreover, even in the ideal delocalization regime the electroweak couplings deviate to some extent from the SM values, which also affects the size of the electroweak background processes. The overall effects are twofold (cf. fig. 4): on one hand the total height of the background shoulder is reduced, whereas on the other hand there is a pronounced interference in the resonance region with a sign change at m' . In order to compute significances, it is therefore sensible to compare the signal samples with respective samples generated in the ideal delocalization setup rather than a SM sample, thus accounting for any model effects except for resonant W' diagrams. This approach is justified by the fact pointed out above that, in any case, the Z' must be assumed to have already been discovered at the eve of a 3SHLM-like W' search.

As illustrated in fig. 6, despite its overall tiny cross sections the purely leptonic channel turns out to be the most promising one for a direct W' search compared to the results of the semileptonic channels stated in the previous sections. In fact, depending on the point chosen in parameter space, one of the multi-purpose experiments at the LHC might be 5σ -sensitive to the W' as soon as an integrated luminosity of about $\int L = 10 \text{ fb}^{-1}$ with $\sqrt{s} = 14 \text{ TeV}$ is collected ($m' = 500 \text{ GeV}$, max. $g_{W'ff}$ allowed). On the other hand, fig. 6 also implies that $\int L \lesssim 150 \text{ fb}^{-1}$ would be necessary to cover the entire allowed parameter space of the non-ideally delocalized 3SHLM with a direct W' search at 3σ c. l. ($m' = 600 \text{ GeV}$, min. $g_{W'ff}$ allowed). Note that for $m' = 380 \text{ GeV}$ the minimal allowed $g_{W'ff}$ depends on the choice of M , which could be as low as $\sim 2 \text{ TeV}$ [21]. However, anything below the value of 3.5 TeV would make the heavy fermions visible in the respective search channels [30]. Therefore we only consider higher values.

IV. SUMMARY

Besides the Higgs mechanism, various different approaches exist to describe the spontaneous breaking of the electroweak symmetry, for example through the introduction of one (or more) additional compact space-time dimension rather than a new field. New gauge

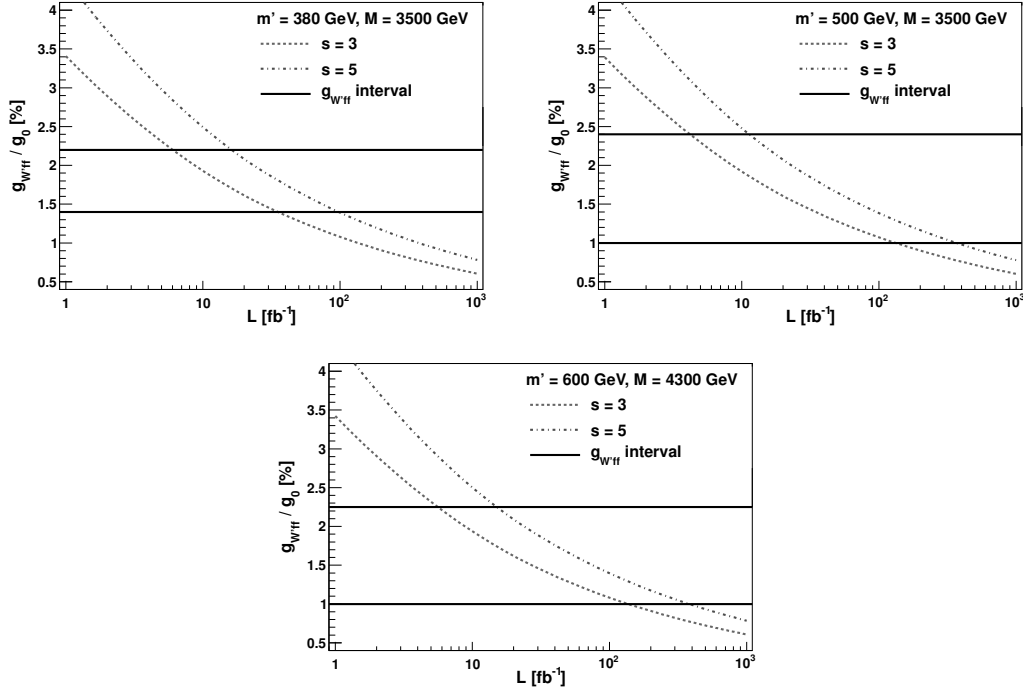


FIG. 6: $s = 3$ and $s = 5$ sensitivity contours for a direct W' search in the $\ell\nu\ell\ell$ channel at detector level, depending on the available integrated luminosity and the $g_{W'ff}$ value. The values of M have been chosen as low as possible while complying with the bounds of [21] and demanding that the heavy fermions remain undetected in their respective search channels [30]. Increasing M generally shifts all $g_{W'ff}$ windows to larger values, thus improving detection as well as exclusion prospects.

degrees of freedom emerge naturally from the necessity to gauge the whole 5D bulk, which can then be used to dynamically break the symmetry, e. g. by assigning non-trivial vacuum configurations to these gauge components. The Three-Site Higgsless Model [14] represents a minimal approach in this respect, since the extra dimension is discretized on only three sites, thus eliminating all higher Kaluza-Klein excitations except for the two lightest sets from the spectrum. In this setup, the heavy copies of the W and the Z constitute the most accessible signatures of the new physics.

Since discovery thresholds for the Z' of the 3SHLM in the ideal delocalization scenario at the LHC with $\sqrt{s} = 14$ TeV have been published recently [32] (cf. also [42]), this study is focussed on the discovery potential of the model-specific W' in the non-ideally delocalized scenario [21, 23], using it as a discriminative signature against other models with heavy neutral resonances as well as against the ideally delocalized scenario of the 3SHLM, where

the s -channel signal of the W' must also vanish. To that end, the signal as well as dominating backgrounds with final state signatures $\ell\ell jj$, $\ell\nu jj$ and $\ell\nu\ell\ell$ (dropping the hadronic final state $jjjj$ because of the huge QCD backgrounds) were generated with the parton-level MC event generator WHIZARD [38], showered with PYTHIA [39] and finally processed with the generic detector simulation software DELPHES [40] mimicking the setup of the ATLAS experiment at the LHC.

All three channels were then examined with respect to their discovery prospects of a W' , also testing a statistical method introduced in [23] to disentangle the W' from the degenerate Z' in the $\ell\nu jj$ channel at the detector level. It was found that the $\ell\ell jj$ channel provides such a poor signal-to-background ratio that a discovery within a reasonable amount of LHC data appears to be out of reach even at the most promising point in the parameter space of the non-ideally delocalized scenario. This is even more true for the $\ell\nu jj$ channel after applying the said method to numerically disentangle the W' and Z' signals, although the fact that afterwards the W' significance drops indeed to nearly zero in ideal delocalization whereas a residual significance remains in non-ideal delocalization can be considered as a proof-of-method.

In the end, despite its tiny overall cross sections, the $\ell\nu\ell\ell$ channel remains as the only one with realistic discovery prospects for the W' in the non-ideally delocalized 3SHLM with sensible assumptions on LHC runtime and luminosity. In fact, at the most promising parameter point, i. e. $m' = 500$ GeV and maximal $g_{W'ff}$ allowed within the model scenario, a 5σ discovery might already be possible with $\int L \sim 10 \text{ fb}^{-1}$, which is indeed only little more than the 8 fb^{-1} reported in [32] to be necessary for the discovery of the ideally delocalized Z' in the $\ell\nu jj$ channel. We obtain comparable if somewhat larger amounts of reducible QCD background. However, the non-ideal delocalization also lowers the discovery threshold for the total degenerate W'/Z' signal in the $\ell\nu jj$ channel, so that in this scenario—with the most optimistic choice of the parameters m' and $g_{W'ff}$ —a respective discovery may already be expected around $\int L \sim 5 \text{ fb}^{-1}$ at $\sqrt{s} = 14 \text{ TeV}$ according to the present study.

Since the coupling $g_{W'ff}$ is also bounded from below in the non-ideally delocalized scenario, it is in principle possible to completely exclude this scenario via a direct W' search. It turns out that $\int L \lesssim 150 \text{ fb}^{-1}$ of LHC data would be required for a complete 3σ exclusion, so that in summary, on the basis of the present study, an s -channel search for the W' with final state $\ell\nu\ell\ell$ may be considered a feasible approach to cover the entire parameter space of

the non-ideally delocalized 3SHLM within a realistic LHC runtime. Clearly, it could pay off to also look for different, possibly more sensitive approaches for an exclusion of the 3SHLM in the presence of a Z' -like resonance, for example a precise enough determination of the suppressed Z' coupling to SM fermions $g_{Z'ff}$, which is essentially fixed by m' within the 3SHLM. The extraction of liable exclusion bounds in this case could be a topic of further studies.

* fabian.bach@physik.uni-wuerzburg.de

† ohl@physik.uni-wuerzburg.de

- [1] D. Dicus and V. Mathur, Phys.Rev. **D7**, 3111 (1973).
- [2] J. M. Cornwall, D. N. Levin, and G. Tiktopoulos, Phys.Rev.Lett. **30**, 1268 (1973).
- [3] J. M. Cornwall, D. N. Levin, and G. Tiktopoulos, Phys.Rev. **D10**, 1145 (1974).
- [4] B. W. Lee, C. Quigg, and H. Thacker, Phys.Rev.Lett. **38**, 883 (1977).
- [5] B. W. Lee, C. Quigg, and H. Thacker, Phys.Rev. **D16**, 1519 (1977).
- [6] M. S. Chanowitz and M. K. Gaillard, Nucl.Phys. **B261**, 379 (1985).
- [7] P. W. Higgs, Phys.Lett. **12**, 132 (1964).
- [8] P. W. Higgs, Phys.Rev.Lett. **13**, 508 (1964).
- [9] S. Weinberg, Phys.Rev. **D13**, 974 (1976).
- [10] S. Dimopoulos and L. Susskind, Nucl.Phys. **B155**, 237 (1979).
- [11] L. Randall and R. Sundrum, Phys.Rev.Lett. **83**, 3370 (1999), hep-ph/9905221.
- [12] J. M. Maldacena, Adv.Theor.Math.Phys. **2**, 231 (1998), hep-th/9711200.
- [13] J. M. Maldacena, Int.J.Mod.Phys. **A15S1**, 840 (2000), hep-ph/0002092.
- [14] R. Chivukula, B. Coleppa, S. Di Chiara, E. H. Simmons, H.-J. He, et al., Phys.Rev. **D74**, 075011 (2006), hep-ph/0607124.
- [15] N. Arkani-Hamed, A. G. Cohen, and H. Georgi, Phys. Rev. Lett. **86**, 4757 (2001), hep-th/0104005.
- [16] C. T. Hill, S. Pokorski, and J. Wang, Phys. Rev. **D64**, 105005 (2001), hep-th/0104035.
- [17] H. Georgi, Phys.Rev.Lett. **63**, 1917 (1989).
- [18] H. Georgi, Nucl.Phys. **B331**, 311 (1990).
- [19] M. Bando, T. Kugo, and K. Yamawaki, Phys.Rept. **164**, 217 (1988).

- [20] M. Harada and K. Yamawaki, Phys.Rept. **381**, 1 (2003), hep-ph/0302103.
- [21] T. Abe, S. Matsuzaki, and M. Tanabashi, Phys.Rev. **D78**, 055020 (2008), 0807.2298.
- [22] T. Abe, R. Chivukula, N. D. Christensen, K. Hsieh, S. Matsuzaki, et al., Phys.Rev. **D79**, 075016 (2009), 0902.3910.
- [23] T. Ohl and C. Speckner, Phys. Rev. **D78**, 095008 (2008), 0809.0023.
- [24] H.-J. He et al., Phys. Rev. **D78**, 031701 (2008), 0708.2588.
- [25] J.-G. Bian et al., Nucl. Phys. **B819**, 201 (2009), 0905.2336.
- [26] T. Han, D. Krohn, L.-T. Wang, and W. Zhu, JHEP **03**, 082 (2010), 0911.3656.
- [27] T. Han, H.-S. Liu, M.-X. Luo, K. Wang, and W. Wu, Phys.Rev. **D80**, 095010 (2009), 0908.2186.
- [28] M. Asano and Y. Shimizu, JHEP **01**, 124 (2011), 1010.5230.
- [29] G. Brooijmans et al. (New Physics Working Group), pp. 191–380 (2010), 1005.1229.
- [30] C. Speckner, Ph.D. thesis, Würzburg University (2010), 1011.1851.
- [31] E. Accomando, D. Becciolini, S. De Curtis, D. Dominici, and L. Fedeli (2011), 1107.4087.
- [32] T. Abe, T. Masubuchi, S. Asai, and J. Tanaka, Phys.Rev. **D84**, 055005 (2011), 1103.3579.
- [33] R. Casalbuoni, S. De Curtis, D. Dominici, and R. Gatto, Phys.Lett. **B155**, 95 (1985).
- [34] K. Hagiwara, R. D. Peccei, D. Zeppenfeld, and K. Hikasa, Nucl. Phys. **B282**, 253 (1987).
- [35] ALEPH Collaboration, DELPHI Collaboration, L3 Collaboration, OPAL Collaboration, SLD Collaboration, LEP Electroweak Working Group, SLD Electroweak Group, SLD Heavy Flavour Group, Phys. Rept. **427**, 257 (2006), hep-ex/0509008.
- [36] R. Chivukula, E. H. Simmons, H.-J. He, M. Kurachi, and M. Tanabashi, Phys.Rev. **D72**, 015008 (2005), hep-ph/0504114.
- [37] G. Aad et al. (ATLAS) (2009), 0901.0512.
- [38] W. Kilian, T. Ohl, and J. Reuter, Eur.Phys.J. **C71**, 1742 (2011), 0708.4233.
- [39] T. Sjostrand, S. Mrenna, and P. Z. Skands, JHEP **0605**, 026 (2006), hep-ph/0603175.
- [40] S. Oryn, X. Rouby, and V. Lemaitre (2009), 0903.2225.
- [41] M. Cacciari, G. P. Salam, and G. Soyez, JHEP **0804**, 063 (2008), 0802.1189.
- [42] F. Bach, Master’s thesis, Würzburg University (2009).